Mechanisms of long-lasting hyperpolarizations underlying slow sleep oscillations in cat corticothalamic networks

Diego Contreras, Igor Timofeev and Mircea Steriade*

Laboratoire de Neurophysiologie, Faculté de Médecine, Université Laval, Québec, Canada G1K 7P4

1. To explore the nature of the long-lasting hyperpolarizations that characterize slow oscillations in corticothalamic circuits *in vivo*, intracellular recordings were obtained under ketamine–xylazine anaesthesia from cortical (Cx) cells of the cat precruciate motor cortex, thalamic reticular (RE) cells from the rostrolateral sector, and thalamocortical (TC) cells from the ventrolateral (VL) nucleus.

2. Measurements in the three cell types showed input resistance (R_{in}) to be highest during the long-lasting hyperpolarizations that correspond to depth-positive waves of the cortical EEG. R_{in} was lowest during the early phase of high-amplitude depth-negative EEG waves and increased thereafter until the next cycle of the slow oscillation.

3. Spontaneous long-lasting hyperpolarizations were compared with those evoked by dorsal thalamic stimulation. Voltage *versus* current (V–I) plots showed similar membrane potential (V_m) ranges and slopes for spontaneous and evoked hyperpolarizations in both Cx and RE cells. V–I plots from TC cells had similar slopes, but V_m during evoked hyperpolarizations was displaced towards more negative values.

4. Intracellular injection of constant hyperpolarizing current in Cx cells increased the amplitude of the initial part of the depolarizing plateau of the slow oscillation, but decreased the amplitude of the last part.

5. These results suggest disfacilitation to be the dominant mechanism in the membrane of cortical and thalamic cells during the spontaneous long-lasting hyperpolarizations, which shape and synchronize slow oscillations in corticothalamic networks. In Cx and RE cells, the same mechanism underlies thalamically evoked long-lasting hyperpolarizations. By contrast, evoked responses in TC cells show a strong additional hyperpolarizing factor. We propose that $GABA_B$ processes are stronger in TC than in Cx neurones, thus rendering the thalamus an easier target for absence-type epileptic phenomena through potentiation of thalamic rebound capabilities.

During the state of resting sleep the electrical activity of the brain is characterized by three types of high-amplitude and low-frequency rhythms, termed spindle (7–14 Hz), delta (1–4 Hz) and slow (< 1 Hz) oscillations. The slow oscillation is generated in neocortical (Cx) neurones and is reflected in thalmic reticular (RE) and thalamocortical (TC) neurones, thus grouping the thalamically generated spindles and clock-like delta rhythm in slowly recurring wave sequences (Steriade, Contreras, Curró Dossi & Nuñez, 1993*b*; Steriade, Nuñez & Amzica, 1993*d*). Intracellular recordings of Cx neurones under various types of anaesthesia showed that the slow oscillation consists of rhythmic depolarizing components separated by prolonged (0·2–0·8 s) hyperpolarizations (Steriade, Nuñez & Amzica, 1993*c*). In all investigated cortical and thalamic cellular types, the long-lasting hyperpolarization and silenced neuronal firing are related to prolonged depth-positive waves in the cortical electroencephalogram (EEG), a stigmatic feature of the slow oscillation during both ketamine–xylazine anaesthesia (Contreras & Steriade, 1995) and natural sleep (Steriade, Amzica & Contreras, 1996). While Cx, RE and TC cells recorded from naturally sleeping animals display spike trains or spike bursts separated by exceedingly long-lasting periods of silence, the same neurones exhibit tonic firing patterns during states of brain arousal (Evarts, 1964; Steriade, Deschênes & Oakson, 1974; McCarley, Benoit & Barrionuevo, 1983; Steriade, Domich & Oakson, 1986).

The mechanisms underlying the long-lasting hyperpolarizations of Cx, RE and TC neurones have not yet been elucidated. Three main factors should be considered, as

* To whom correspondence should be addressed.

follows. (i) In the initial study that described the slow cortical oscillation, intracellular infusion of Cl^- reduced the amplitude and duration of the cyclic and prolonged hyperpolarizations (Steriade *et al.* 1993*c*). However, the relatively short $GABA_A$-mediated inhibitory postsynaptic potentials (IPSPs) in neocortical neurones (Kelly, Krnjevic, Morris & Yim, 1969; Connors, Malenka & Silva, 1988) cannot account for the whole duration of the prolonged hyperpolarizations. Further evidence that local circuit GABAergic cortical neurones do not play a crucial role in the genesis of prolonged hyperpolarizations is provided by the fact that out of more than a thousand cortical neurones only one discharged in close temporal relation with the long-lasting hyperpolarizations of the other neurones (Steriade, Contreras & Amzica, 1994). Moreover, intracellularly recorded and morphologically identified aspiny basket (presumably inhibitory) cells oscillate in phase with pyramidally shaped neurones during both the depolarizing and hyperpolarizing components of the slow oscillation (Contreras & Steriade, 1995). (ii) Other possible mechanisms contributing to the long-lasting hyperpolarizations, which follow prolonged depolarizations and trains of action potentials in neocortical neurones, are a series of intrinsic voltage-, Na^+- and Ca^{2+}-dependent K^+ currents (Halliwell, 1986; Schwindt, Spain, Foehring, Stafstrom, Chubb & Crill, 1988; Schwindt, Spain & Crill, 1989). Indeed setting the cholinergic mesopontine and basalis circuits into action leads to suppression of long-lasting hyperpolarizations in Cx neurones, disruption of the slow oscillation and its replacement by tonic firing, an effect that is abolished by blockers of muscarinic receptors (Steriade, Amzica & Nuñez, 1993*a*). It is known that activation of muscarinic receptors results in the inhibition of slow calcium- and sodium-activated potassium currents ($I_{K(Ca)}$ and $I_{K(Na)}$, respectively) (Schwindt *et al.* 1989). (iii) Another important factor contributing to the long-lasting hyperpolarizations would be the withdrawal of excitatory activity in corticothalamic networks, thus leading to a generalized disfacilitation (Steriade *et al.* 1994; Contreras & Steriade, 1995). This proposal was based on the disappearance of synaptic activity during the late phase of the prolonged hyperpolarization (for example see Fig. 3*B* in Steriade *et al.* 1993*c*).

On the other hand, the prolonged depth-positive EEG waves and the corresponding long-lasting hyperpolarizations that characterize the spontaneous slow oscillation are almost identical to those evoked by thalamic or cortical stimulation. Evoked hyperpolarizations have been shown to correspond to biphasic $GABA_A$–$GABA_B$ IPSPs in *in vitro* studies from thalamic (Crunelli, Haby, Jassik-Gerschenfeld, Leresche & Pirchio, 1988) and cortical (Connors *et al.* 1988) slices.

In order to shed further light onto the processes underlying slow oscillatory behaviour in corticothalamic networks we have studied the evolution of membrane input resistance (R_{in}) during various phases of the slow oscillation and compared spontaneous long-lasting hyperpolarizations with those evoked by thalamic stimulation.

METHODS

Experiments were carried out on adult cats (2·5–3·5 kg) anaesthetized with ketamine–xylazine (10–15 and 2–3 mg kg^{-1}, respectively, I.M.). In addition, all pressure points and tissues to be incised were infiltrated with lidocaine (lignocaine). Animals were paralysed with gallamine triethiodide (33 mg kg^{-1} I.V.) once the EEG indicated the onset of deep anaesthesia. After mounting in stereotaxic apparatus, animals were artificially ventilated (end-tidal CO_2, 3·5–3·7%). To assess the depth of anaesthesia, heart rate (acceptable range, 90–110 beats min^{-1}) and EEG (high-amplitude and low-frequency waves) were continuously monitored and kept constant. Additional doses of anaesthetic (3–7 mg kg^{-1}) were administered as necessary (2–3 times during the experiment). Body temperature was maintained at 37–39 °C. Glucose saline (5% glucose, 10 ml I.P.) was given 2 or 3 times during the experiments, which lasted on average between 8 and 10 h. At the end of all experiments the cats were given a lethal dose of pentobarbitone.

Recording and stimulation

For cortical intracellular recordings the surface of the pericruciate area was exposed, after resection of the overlying bone and dura mater, and bathed in mineral oil to prevent desiccation. For thalamic intracellular recordings the surface of the cortex that corresponds to the anterior half of the marginal and suprasylvian gyri was cauterized with silver nitrate. The cortex and white matter were removed by suction until the head of the caudate nucleus was exposed. Micropipettes were then lowered through the head of the caudate nucleus in order to reach the rostrolateral sector of the RE nucleus and the ventrolateral (VL) thalamic nucleus (A12, L3, D3, stereotaxic co-ordinates).

The stability of the recordings was improved by performing a bilateral pneumothorax, drainage of the cisterna magna, hip suspension, and filling of the holes made for recording with a solution of 4% agar.

The gross EEG was recorded monopolarly by means of a screw inserted into the bone over the pericruciate cortex, contralateral to the side of cellular recordings. The focal EEG was recorded via coaxial electrodes (0·2 mm tip exposure, 0·6 mm tip separation) which were placed in the lateral part of the precruciate gyrus (motor cortex, area 4); the depth was adjusted to obtain an inverse polarity of the thalamically evoked potential. In all monopolar recordings the indifferent electrode was placed on the neck muscles.

Stimulating coaxial electrodes were placed in the VL nucleus and the cerebellothalamic pathway (brachium conjunctivum, BC) according to conventional stereotaxic coordinates (P2, L2·5, D−1·5). Stimulation was also performed by means of the cortical coaxial electrodes used for EEG recording.

Intracellular recordings were performed with glass micropipettes filled with a solution of 3 M potassium acetate and DC resistances of 35–45 MΩ. The pipettes for intracellular recordings in the cortex were placed about 1 mm apart from the coaxial EEG recording electrodes; the depth of insertion was read from the micromanipulator. Estimation of neuronal depth had an error of less than 15% when compared with the location of intracellularly stained neurones (Contreras & Steriade, 1995). A high-impedance amplifier (bandpass, 0–5 kHz) with active bridge circuitry was used to record and inject current into the cells. The signals were recorded on an eight-channel tape with bandpass of 0–9 kHz and digitized at 20 kHz for off-line computer analysis.

RESULTS

Data base and neuronal identification

Intracellular recordings, with stable resting membrane potential (V_m) more negative than −55 mV and overshooting action potentials, were obtained from fifty-two Cx neurones, twenty-one RE neurones and fifty TC neurones. All Cx cells had the characteristics of regularly spiking cells (McCormick, Connors, Lighthall & Prince, 1985) and were located in the precruciate motor cortex from layers II to VI. RE neurones were recorded from the rostrolateral sector and TC cells from the VL nucleus. Cells

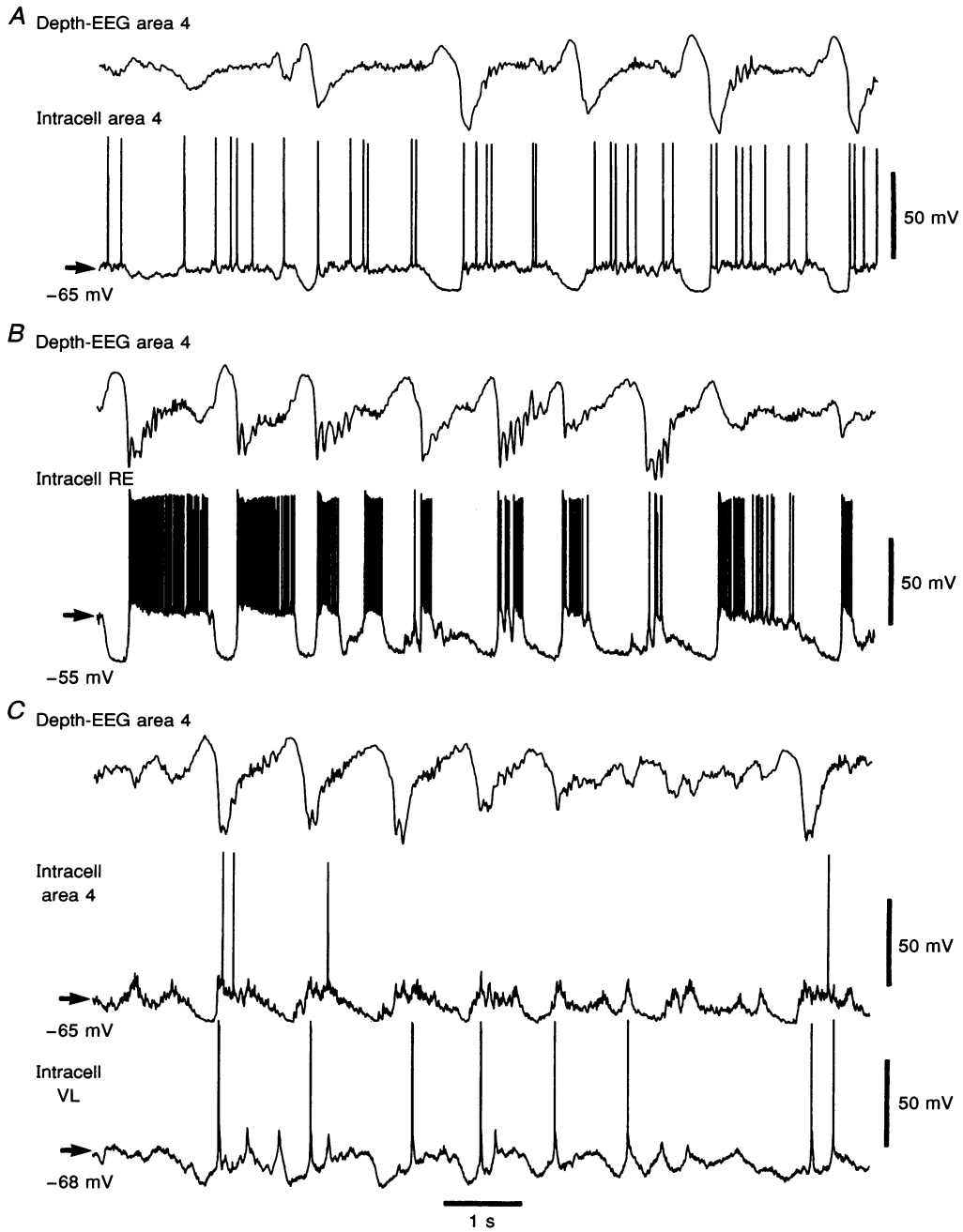

Figure 1. Spontaneous slow oscillations in cortical and thalamic neurones under ketamine–xylazine anaesthesia

A, *B* and *C*, examples of spontaneous activity recorded intracellularly from a motor cortical cell (Intracell area 4 in *A*); an RE cell (Intracell RE in *B*) from the rostrolateral sector; and a double impalement (in *C*) of a motor cortical (Intracell area 4) and a TC cell from VL (Intracell VL), recorded simultaneously with the corresponding EEG from the depth of the motor cortex (Depth-EEG area 4, in *A–C*). All cells followed the characteristic EEG components of the slow oscillation, hyperpolarizing in phase with long-lasting depth-positive EEG waves. All cells are depicted at their resting V_m levels. In this and subsequent figures, V_m is indicated at arrows. Polarity of EEG recordings is as for intracellular recordings (positivity upwards).

displayed monosynaptic (TC) or bisynaptic (Cx and RE) responses to the stimulation of the cerebellothalamic pathway. RE cells were also identified by their prolonged spike bursts and 'accelerando-decelerando' bursting pattern during spontaneous oscillatory activity (Domich, Oakson & Steriade, 1986), or evoked by cortical or dorsal thalamic stimulation.

Spontaneous activity

Under ketamine–xylazine anaesthesia the three cell types and the EEG from the depth of the motor cortex displayed a spontaneous slow oscillatory pattern (Fig. 1) which has previously been described in detail (Steriade *et al.* 1993 *b–d*; Contreras & Steriade, 1995). Briefly, EEG complexes consisted of long-lasting (0·2–0·8 s) depth-positive waves followed by depth-negative waves, repeated at frequencies below 1 Hz. Often the depth-negative waves included oscillations within the frequency range of spindles (7–14 Hz; see Fig. 1*B*) or at higher frequencies (Contreras & Steriade, 1995; Steriade *et al.* 1996). During the depth-positive EEG waves the three types of cell showed a hyperpolarization of V_m (Fig. 1). During the depth-negative waves, Cx and RE cells showed a depolarizing plateau with superimposed oscillatory behaviour at the frequency of spindling or higher, while TC cells displayed IPSPs in the frequency range of spindling, occasionally leading to generation of spike bursts (Fig. 1*C*; see also Fig. 8).

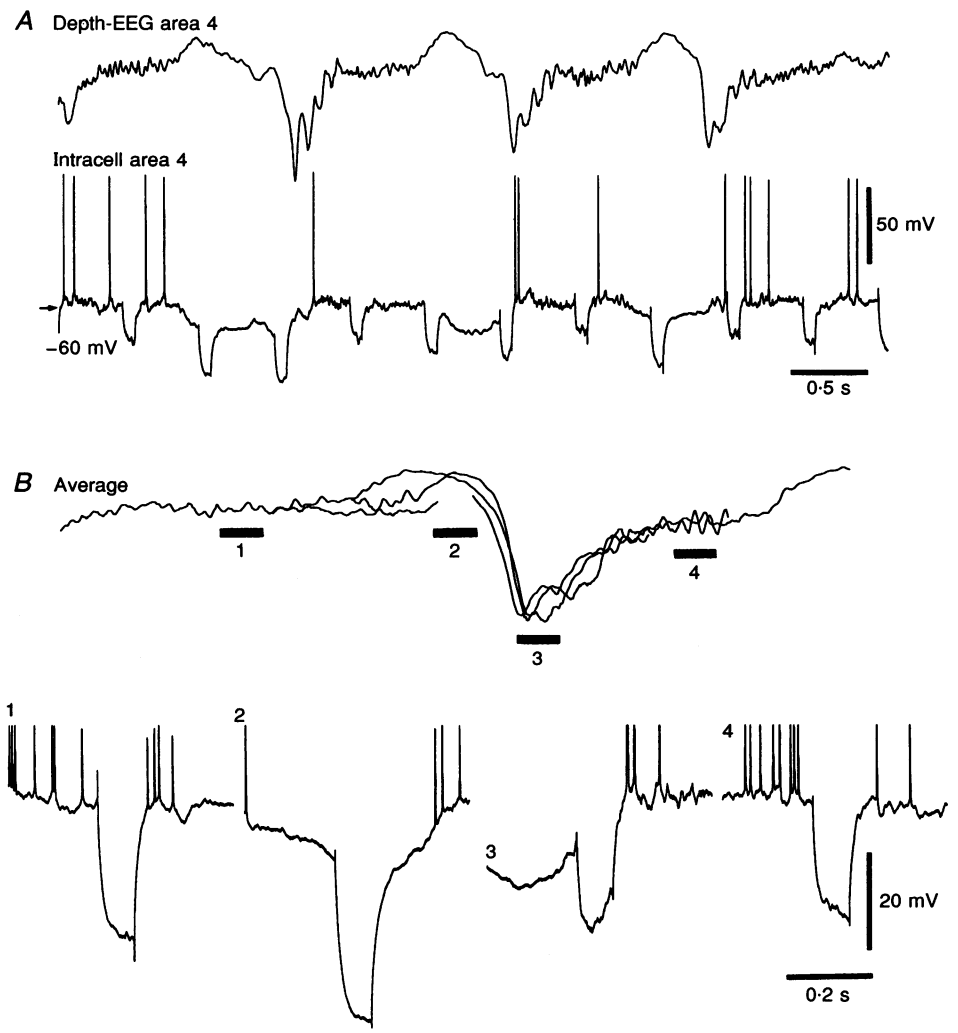

Figure 2. R_{in} increases in cortical cells during depth-positive EEG waves of the slow oscillation

A, a motor cortical cell (Intracell area 4) was recorded together with the depth-EEG from its vicinity (around 1 mm). Square current pulses of 1 nA were applied every 0·5 s while the cell oscillated spontaneously. Changes in apparent R_{in} were reflected by changes in the amplitudes of voltage deflections elicited by pulses. The highest R_{in} was attained during the depth-positive waves, and the lowest during the depth-negative waves. *B*, upper panel shows a superimposition of fragments of the spontaneously oscillating EEG, extracted around the times when pulses were applied and then positioned to constitute an 'average' cycle of the oscillation. Horizontal bars 1–4 in the upper panel indicate the timing of the pulses; the corresponding averaged responses ($n = 5$) are depicted below.

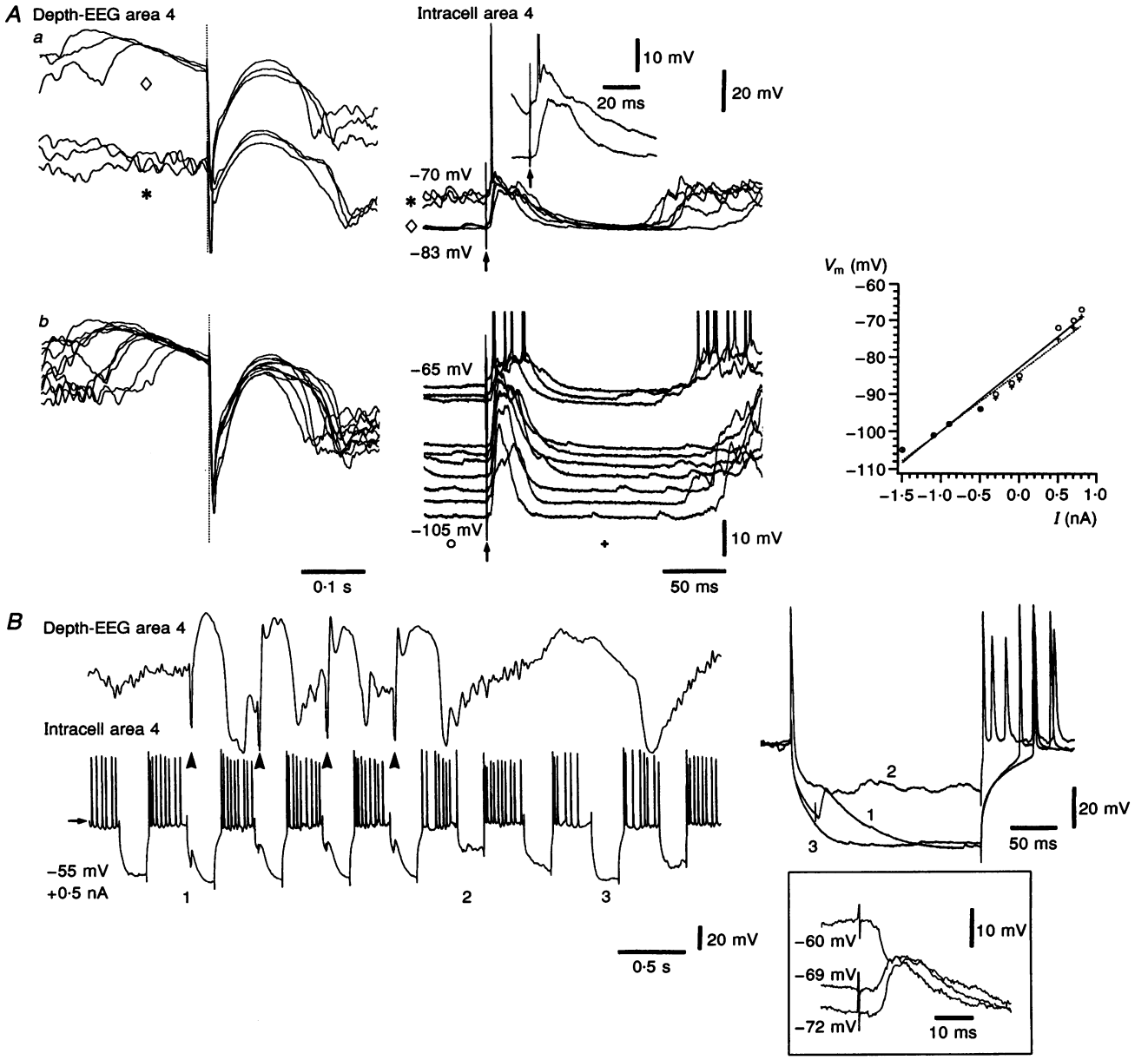

Figure 3. The membrane of cortical cells behaves similarly during spontaneous and evoked depth-positive waves

A a and *A b*, left panels show the corresponding depth-EEGs (Depth-EEG area 4) from the vicinity of the motor cortical cell (Intracell area 4) shown to the right. *A a*, six stimuli of constant parameters were applied to the VL nucleus, three during spontaneous depth-positive waves of the EEG (upper traces, ◇) and three during periods of relative activation of the EEG (lower traces, ∗). The variations in V_m prior to the stimulus are spontaneous. All stimuli induced a similar depth-positive wave in the EEG and a cellular hyperpolarization, regardless of the preceding activity. Variation in V_m did not change the level reached by the hyperpolarization, but changed the amplitude of the initial EPSP and its likelihood of triggering action potentials (*A a*, inset). *A b*, all stimuli were applied during spontaneously occurring depth-positive waves while displacing the V_m of the cell with DC injection. Right panel, V_m values preceding the shock (○) and those during the evoked hyperpolarization (+) are plotted against DC level. *B*, a cortical cell (Intracell area 4) was recorded simultaneously with the depth-EEG from its vicinity. Square hyperpolarizing current pulses (1, 2 and 3) of 1 nA were applied at a depolarized V_m while the cell oscillated spontaneously or responded to thalamic stimulation. The increase in R_{in} during the depth-positive EEG wave is shown in the inset to the right by comparing the response elicited by pulse 2 (during a period of depth-negative waves) with the response elicited by pulse 3 (during the depth-positive EEG wave). When thalamic stimuli were applied during pulse 1 (arrowheads), the voltage deflection was similar to that occurring during the spontaneous depth-positive wave. Most of the initial response elicited by the thalamic stimulus in pulse 1 is an inverted fast IPSP as can be seen in the inset. When the stimulus was applied at more depolarized potentials (−60 mV), it elicited a hyperpolarizing fast IPSP. Action potentials were truncated in *A a* (inset) and in *A b*.

Cortical cells

To determine the variations in R_{in} during the different components of the slow oscillation, we applied hyperpolarizing pulses of constant amplitude throughout the oscillatory cycle ($n = 20$). In Fig. 2*A* a motor cortical cell oscillated spontaneously at around 0·7 Hz and hyperpolarizing pulses of 80 ms and 1 nA were applied every 0·5 s. The responses to pulses were then grouped according to their timing with respect to an oscillatory cycle, indicated by horizontal bars 1–4 in Fig. 2*B*, and averaged. The averaged responses showed that the apparent R_{in} reached its highest value (about 33 MΩ) during the depth-positive phase of the oscillation (Fig. 2*B* 2), whereas before the depth-positive wave (Fig. 2*B* 1) R_{in} was 28 MΩ. During the initial part of the depth-negative EEG waves (Fig. 2*B* 3) the R_{in} dropped to its lowest value (11 MΩ) and thereafter increased (24 MΩ in Fig. 2*B* 4) towards the next depth-positive phase.

In order to compare the behaviour of the membrane between the spontaneous and the thalamically evoked hyperpolarizations, we constructed *V–I* plots ($n = 12$). The V_m of the cells oscillated continuously so that there was not a real resting state, the V_m level being related to the fluctuations in EEG activity. This is shown in Fig. 3*A a*, in a cortical cell in which the V_m before the thalamic stimulation varied spontaneously, as a function of the EEG components. The V_m was hyperpolarized to −83 mV if depth-positive EEG waves preceded the stimulation (diamond in Fig. 3*A a*, left panel) and was depolarized to −70 mV if fast rhythms were in the EEG before the stimulation (asterisk in Fig. 3*A a*, left panel). Spontaneous depolarizations related to the slow oscillation switched from subthreshold to suprathreshold the responses to thalamic stimulation (see inset in Fig. 3*A a*, right panel). However, the V_m was set to a constant level after the stimulation, thus corresponding to the constant shape of the thalamically evoked depth-positive EEG wave. We then applied stimuli at different DC levels and selected those responses that occurred during a spontaneous depth-positive wave, so that the V_m before the stimulus could be used as representative of the spontaneous hyperpolarizations (Fig. 3*A b*). In Fig. 3*A b* (left panel), values of V_m before the stimulus (open circles) and during

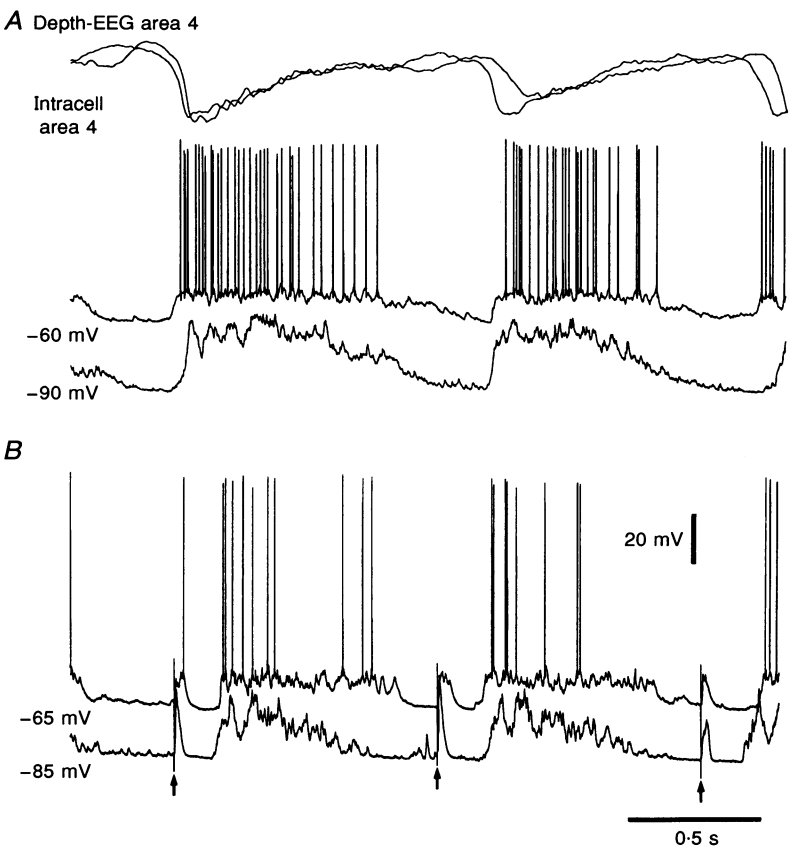

Figure 4. Effect of hyperpolarizing current upon the depolarizing plateau of the spontaneous slow oscillation and of the thalamically evoked postinhibitory depolarizing response

A cortical cell from the motor cortex was recorded intracellularly (Intracell area 4) together with the depth-EEG from its vicinity. *A*, two periods of spontaneous oscillation, without current (at −60 mV) and under −0·5 nA (at −90 mV) are depicted (aligned artificially) together with the corresponding EEGs (top traces). *B*, full responses to two thalamic stimuli (arrows) are depicted at the same DC levels, without current (at −65 mV) and under −0·5 nA (at −85 mV). In both cases the DC hyperpolarization increased the amplitude of the initial part of the depolarizing plateau, but decreased its last part.

the evoked hyperpolarization (crosses) are plotted against the DC level. The *V–I* curves of the evoked and the spontaneous hyperpolarizations had similar slopes (16·1 and 17·0 mV nA^{-1}, respectively) and the same range of V_m, strongly suggesting similar underlying ionic mechanisms.

Figure 3*B* shows, in a different cell, the similarity between the voltage deflections produced by current pulses applied during the spontaneously occurring depth-positive EEG waves (pulse 3) and current pulses applied when the depth-positive waves were induced by thalamic stimulation (pulse 1, arrowheads). It also shows the difference in R_{in} between the depth-negative EEG phase of the oscillation (pulse 2) and the depth-positive EEG phase (pulse 3). An intermediate state between the two is represented by the first pulse of the series (left). Note that all pulses were applied at the same V_m, since by holding the cell with DC depolarizing current (+0·5 nA), spontaneous fluctuations in V_m were almost compensated. The initial response to the thalamic stimulation (arrowheads) was an inverted fast IPSP, as demonstrated by its reversal at around −70 mV during periods of spontaneous depolarization (Fig. 3*B*, inset).

When hyperpolarizing the V_m with DC, the initial part of the depolarizing phase of the oscillation increased in amplitude, as expected for EPSPs, but the last part was decreased in amplitude (Fig. 4). This observation was valid both for the spontaneously occurring oscillatory cycles (Fig. 4*A*) and for those evoked by thalamic stimulation (Fig. 4*B*). Therefore, DC hyperpolarization seems to reveal an underlying progressive decrease in synaptic inputs, with the consequent increase in R_{in} that is observable towards the end of the depolarizing phase of the oscillation. This is supported by the consistent observation of a decrease in firing probability towards the end of the depolarizing phases of the slow oscillation (see upper intracellular traces in Fig. 4*A* and *B*).

RE cells

The first approach to investigate the fluctuations in the apparent R_{in} in RE cells during different components of the slow oscillation was to apply hyperpolarizing pulses at a constant rate of 2 Hz (Fig. 5, pulses indicated by filled circles). Similar to cortical neurones, the voltage deflections produced by pulses had the highest amplitude during the

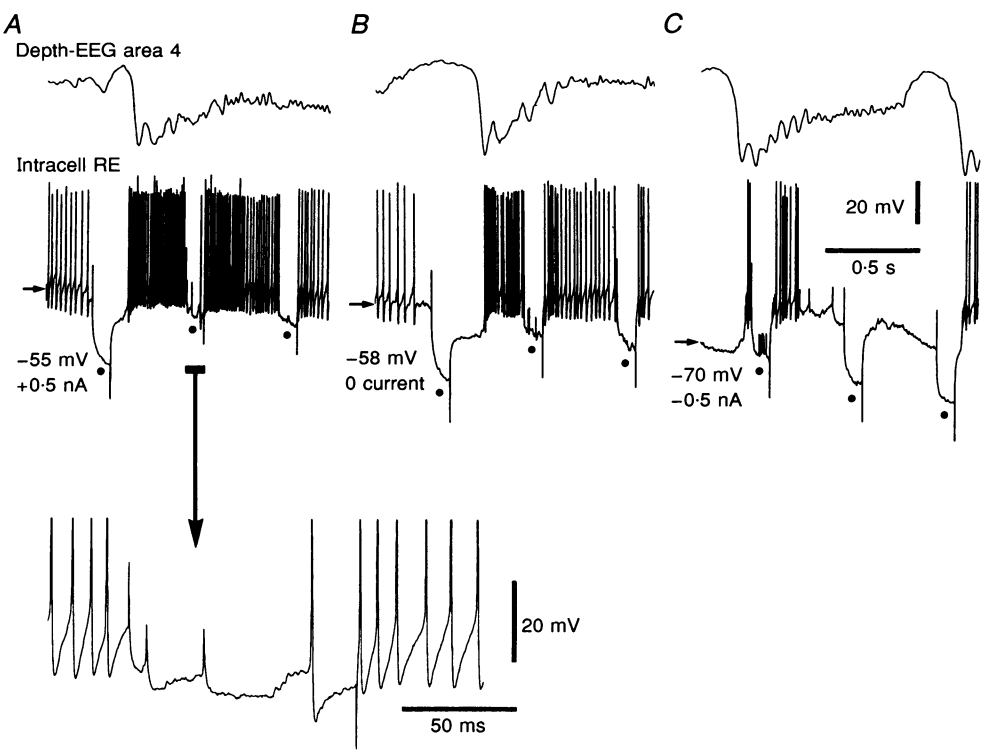

Figure 5. Changes in apparent R_{in} in RE cells during various components of the slow oscillation
A RE cell from the rostrolateral sector (Intracell RE), recorded simultaneously with the corresponding depth-EEG from the motor cortex (Depth-EEG area 4), had its R_{in} tested with hyperpolarizing square current pulses (●) of constant amplitude (1 nA) while the cell oscillated spontaneously. *A*, *B* and *C*, three different cycles of spontaneous oscillation in which the V_m of the cell was changed by DC injection while applying hyperpolarizing pulses. Apparent R_{in} during the depth-positive phase of the EEG reached values of 30–35 MΩ (first pulse in *A* and *B*, third in *C*). During the depth-negative EEG waves, the R_{in} initially dropped to almost negligible values (second pulse in *A* and *B* and first in *C*) and then increased progressively as the oscillation approached the depth-positive phase of the following cycle. Bar and arrow in *A* indicate area of trace expanded below (truncated spikes). Note fast all-or-none spontaneous events resembling dendritic spikes.

depth-positive EEG waves (first of three pulses in Fig. 5*A* and *B*, third in Fig. 5*C*). The responses with lowest amplitudes were elicited with pulses applied during the initial part of the depolarizing phase; occasionally, cell firing occurred during the hyperpolarizing pulse (Fig. 5*A*, expanded portion of trace) due to the high level of synaptic activity in the cell in that phase of the oscillation. Pulses applied further on, closer to the depth-positive phase of the next oscillatory cycle, showed a progressive increase in R_{in} (Fig. 5*A*–*C*). In the cell shown in Fig. 5, the R_{in} measured from the amplitude of the voltage deflection produced by 1 nA pulses was of about 35 MΩ during the depth-positive phase, either with no current (Fig. 5*B*) or on a background of slight DC depolarization (+0·5 nA, Fig. 5*A*). Under hyperpolarizing DC (−0·5 nA, Fig. 5*C*), R_{in} was around 27 MΩ, probably due to inward rectification (Contreras, Curró Dossi & Steriade, 1993).

Similar to the aspects shown above for Cx cells, the spontaneous long-lasting hyperpolarizations that characterized the slow oscillation in RE cells resembled those evoked by thalamic stimulation in their duration,

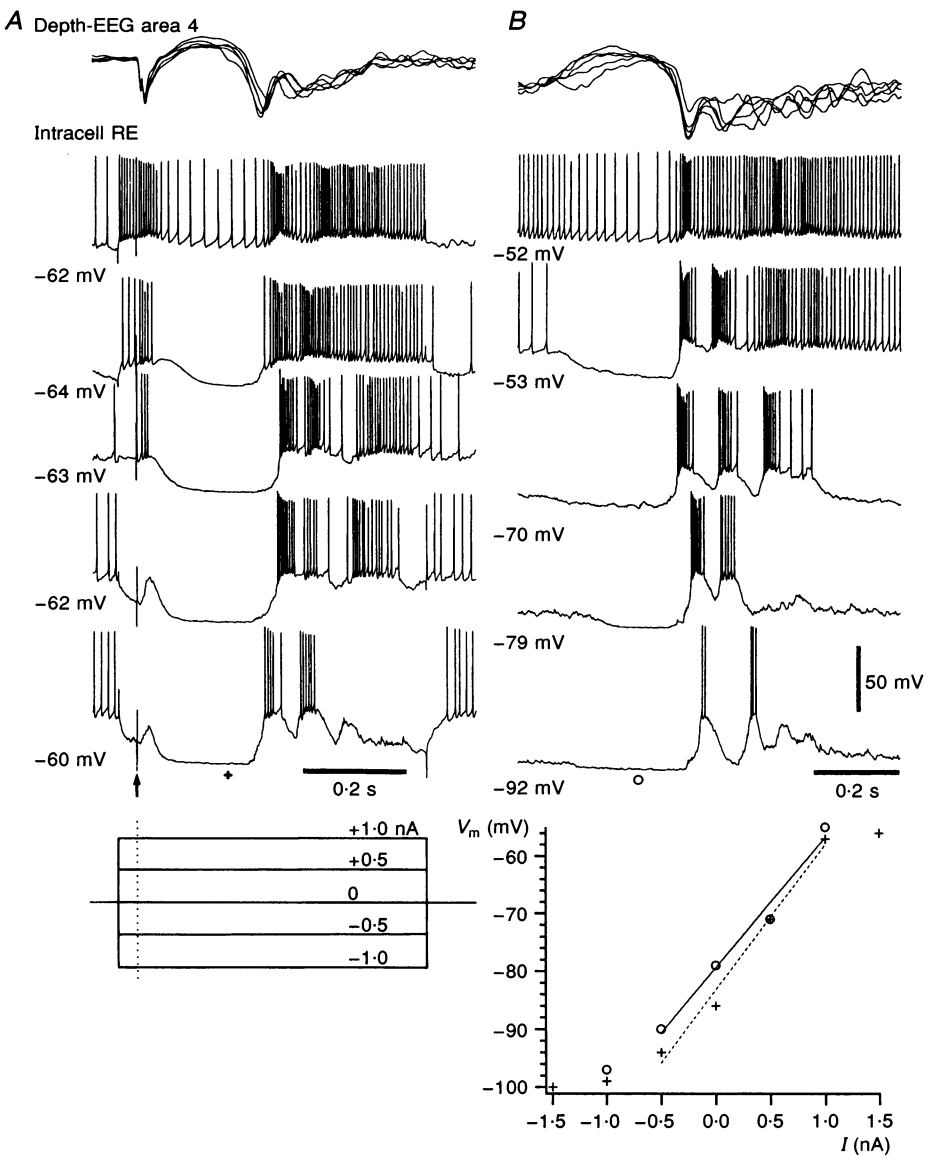

Figure 6. Comparison between spontaneous and evoked hyperpolarizations in RE cells at different V_m levels

A RE cell from the rostrolateral sector (Intracell RE) was recorded simultaneously with precruciate depth-EEG. *A*, a stimulus (arrow) to the dorsal thalamus (VL) was applied during long (590 ms) current pulses with step changing intensities (for currents see bottom panel). Top panel is the superimposition of corresponding responses from depth-EEG. *B*, the cell oscillated spontaneously and its V_m was displaced by DC injection with the same current values as those used for the thalamic stimuli in *A*. The negative peaks from the depth-EEG (superimposed top traces) were used to align all traces. *V*–*I* plots from evoked (+) and spontaneous (○) hyperpolarizations were within the same V_m ranges and showed similar slopes.

amplitude and associated EEG events. In order to compare the spontaneous and evoked events, we studied the behaviour of the RE cell membrane during the hyperpolarization to injected current ($n = 10$). In Fig. 6*A* a thalamic stimulus to the VL nucleus (arrow) was applied during a long (590 ms) current pulse whose amplitude was changed in steps of 0·5 nA (see pulse protocol at the bottom; dotted line represents the stimulus). Approximately the same levels of DC were used in Fig. 6*B* for the spontaneously occurring cyclic hyperpolarizations. The *V–I* curves (Fig. 6) for the evoked (crosses) and the spontaneous hyperpolarization (open circles) showed similar slopes in their linear portions (22·8 and 25·2 mV nA^{-1}, respectively) and V_m ranges. This result suggests that similar ionic mechanisms dominate the behaviour of RE cells during the evoked and the spontaneous long-lasting hyperpolarizations.

TC cells

During the V_m variations related to the slow oscillation, as described above for Cx and RE neurones, TC cells also showed changes in their apparent R_{in} as measured by applying hyperpolarizing pulses of constant amplitude ($n = 20$). Figure 7 shows such a protocol in which the responsiveness of the TC cell was altered by changes in R_{in}. A hyperpolarizing pulse applied at rest, during a phase preceding the depth-positive phase of the cortical EEG (Fig. 7, pulse 1) when the V_m is relatively stable, induced a rebound burst response with three spikes at 250 Hz. When the pulse was applied during the depth-positive phase (Fig. 7, pulse 2), the higher amplitude voltage deflection produced by the pulse gave rise to a more robust rebound response, with six spikes at 400 Hz. The stronger spike inactivation during the burst suggested that the underlying low threshold spike (LTS) was more effective in pulse 2 (Fig. 7). The hyperpolarizing pulse was applied during the depth-negative phase of the oscillation (Fig. 7, pulse 3) and gave rise to a smaller voltage deflection that no longer elicited a rebound burst at its break, but merely a subthreshold LTS. Thereafter, the R_{in} increased during the late depth-negative phase, as shown by the increase in voltage deflection produced by pulse 4 (Fig. 7), that was again capable of eliciting a rebound burst.

As for Cx and RE cells, we compared the spontaneously occurring long-lasting hyperpolarizations in TC cells with those evoked by thalamic stimulation within the VL nucleus, close to the recording electrode ($n = 10$). Figure 8 shows a TC cell that responded to thalamic stimulation with a biphasic IPSP, not preceded by an EPSP (asterisk, Fig. 8*A*, see inset at −54 mV). This response was studied at different DC levels. In Fig. 8*B*, the same cell was studied for different DC levels during the spontaneous oscillation. The *V–I* plots (Fig. 8, bottom right) showed similar slopes for the evoked (14·5 mV nA^{-1}, crosses) and the spontaneous (14·2 mV nA^{-1}, open circles) long-lasting hyperpolarizations. However, contrary to Cx and RE cells, the V_m values reached by the evoked response were clearly displaced towards hyper-

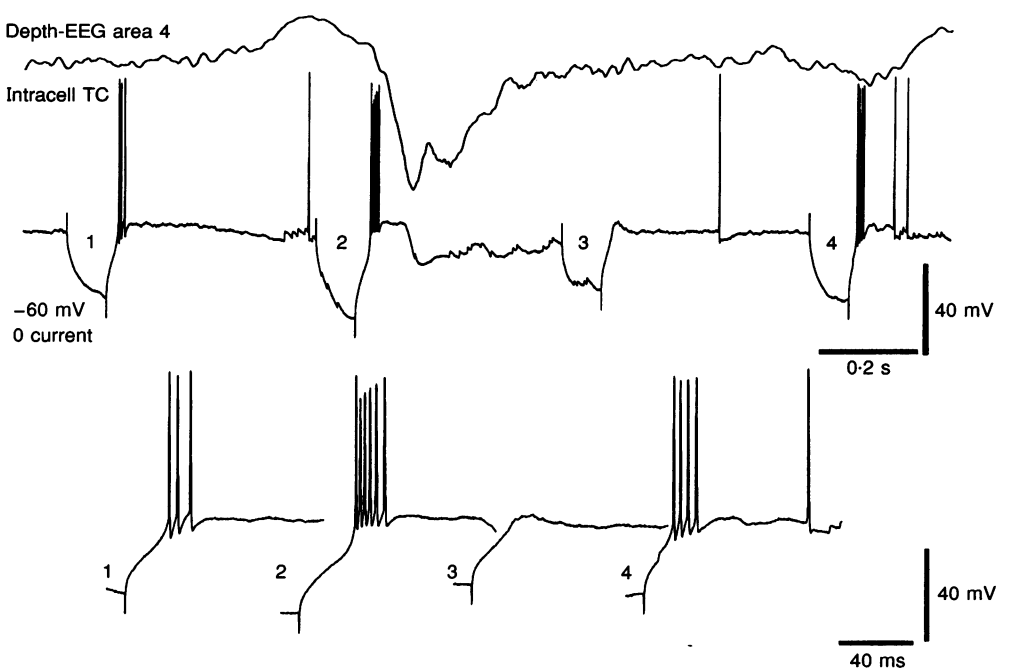

Figure 7. R_{in} changes in TC cells during periods of slow oscillatory behaviour

The responsiveness of a TC cell from VL (Intracell TC), recorded simultaneously with the corresponding motor cortical depth-EEG, was tested with hyperpolarizing pulses (1–4). Maximum voltage deflection and rebound burst response were obtained during the depth-positive EEG wave (detail of the burst expanded below in 2). The smallest voltage deflection which did not trigger a burst, but a subthreshold LTS, was obtained during the depth-negative phase in the EEG (detailed below in 3). The response to pulse 1 was intermediate between pulses 3 and 4.

polarization. This suggests a stronger activation of hyperpolarizing currents during the evoked responses in TC cells. In contrast to the long-lasting hyperpolarization, the V_m during the fast IPSP, either evoked by the thalamic stimulation (Fig. 8*B*) or appearing spontaneously in relation to the sharp negative peaks of the depth-EEG (Fig. 8*A*), showed a linear behaviour with respect to current, with similar small *V–I* slopes (Fig. 8, bottom left plot; 2·2 mV nA^{-1}, evoked, crosses; 2·0 mV nA^{-1}, spontaneous, squares) and voltage ranges. The low R_{in} (as indicated by

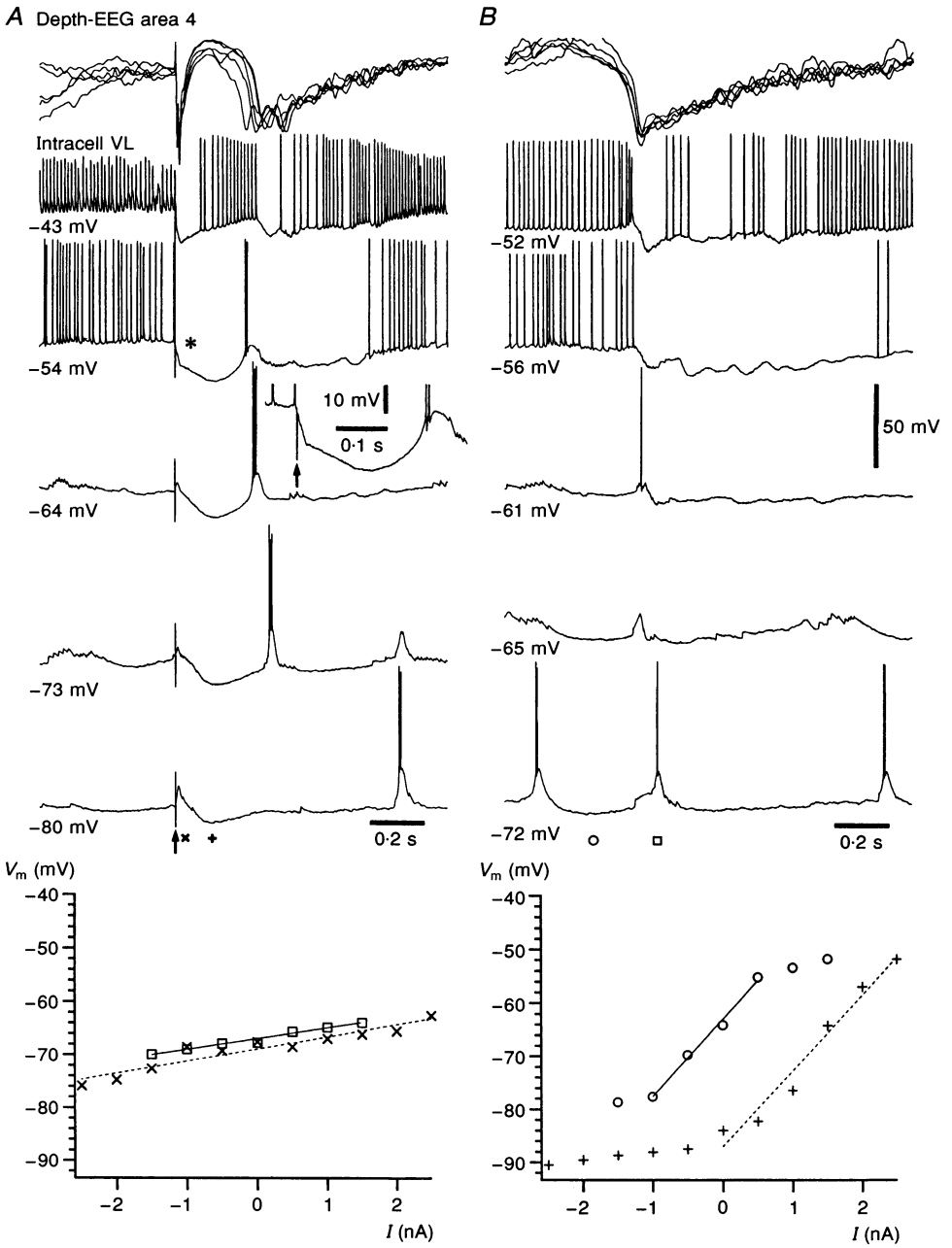

Figure 8. Comparison of spontaneous and evoked hyperpolarizations in TC cells

A TC cell from VL (Intracell VL) was recorded simultaneously with the precruciate depth-EEG. *A*, a stimulus to the dorsal thalamus (VL) was applied (at arrow) during different DC levels (from top to bottom: +2·5, +1·5, 0, −1·5 and −2·5 nA). Top trace is the superimposition of thalamically evoked responses of depth-EEG. The cell responded with a biphasic IPSP to thalamic stimulation (see inset of expanded trace at −54 mV, indicated by arrow). *B*, the cell oscillated spontaneously and its V_m was displaced by DC injection (from top to bottom: +1·5, +0·5, 0, −0·5, −1·5 nA). The sharp negative deflections of the depth-EEG (superimposed top traces) were used to align all traces. *V–I* plots from evoked (×, left plot) and spontaneous (□, left plot) fast IPSP, as well as from evoked (+, right plot) and spontaneous (○, right plot) long-lasting hyperpolarizations, show that while the spontaneous and evoked fast IPSPs were very similar, the evoked long-lasting hyperpolarizations had V_m displaced to hyperpolarizing values.

the slope of the V–I curve), the linear behaviour, and the reversal at around −70 mV (not shown) suggest a chloride GABAergic nature.

DISCUSSION

We obtained two basic results. (i) During the spontaneous slow (< 1 Hz) oscillatory behaviour of Cx, RE and TC cells, the R_{in} fluctuated concomitantly and reached a maximum value, in all of these cell types, during the long-lasting hyperpolarizations that correspond to depth-positive EEG waves. The minimum values were obtained during the early phase of the depth-negative waves, when the EEG consists of high-amplitude rhythms within the frequency range of 7–14 Hz. Thereafter, the R_{in} progressively increased approaching the next cycle, while the EEG waves decreased in amplitude and increased in frequency. We regard this result as suggesting a disfacilitation mechanism in corticothalamic networks, but this interpretation does not exclude the participation of some synaptic or intrinsic currents (see Introduction and below). (ii) V–I plots from spontaneous and evoked hyperpolarizations were similar in both Cx and RE cells. In TC cells, evoked hyperpolarizations were at more hyperpolarized V_m than those occurring spontaneously, although they showed similar slopes.

The cellular activities and the phase relations between Cx, RE and TC cells during the slow oscillation have been previously described (Steriade *et al.* 1993*b–d*; Contreras & Steriade, 1995). In those studies, it was proposed that the major factor accounting for the cyclic hyperpolarizations is the withdrawal of excitatory synaptic currents, or disfacilitation. This was based on the fact that all cells recorded extra- or intracellularly, including intracellularly stained aspiny basket cells (putative inhibitory neurones), fired in the same phase of the oscillation (see Fig. 1 in Contreras & Steriade, 1995). Furthermore, intracellular recordings with pipettes containing CGP 35348, a $GABA_B$ antagonist, did not have any appreciable effect on the oscillation (M. Steriade, A. Nuñez & F. Amzica, unpublished results), and intracellular recordings with Cl^- pipettes showed only a small decrease in the initial part of the hyperpolarizing phase (Steriade *et al.* 1993*c*). These data rule out any important participation of GABA-mediated currents in the spontaneous hyperpolarizations.

However, spontaneous hyperpolarizations looked similar to those evoked by thalamic stimulation in Cx (Fig. 3), RE (Fig. 6) and TC cells (Fig. 8), both in their amplitudes and durations. Also, the corresponding depth-EEG positive waves were strikingly similar in both cases. Since evoked PSPs in neocortical neurones have been extensively studied, both *in vivo* (Stefanis & Jasper, 1964; Pollen & Lux, 1965; Renaud, Kelly & Provini, 1974; Nuñez, Amzica & Steriade, 1993) and *in vitro* (Avoli, 1986; Connors *et al.* 1988; McCormick, 1989) we compared the two (spontaneous and evoked) hyperpolarization processes in order to gain insight into the underlying mechanisms.

Cortical cells

Evoked IPSPs in Cx cells *in vitro* have been demonstrated to be mediated by $GABA_A$ and $GABA_B$ receptors, giving rise to a fast IPSP with short latency and duration, associated with a large increase in membrane conductance, followed by a longer lasting, smaller amplitude IPSP, with a relatively small conductance increase (Connors *et al.* 1988). Evoked responses *in vivo* are more complex and consist of EPSPs, followed by a fast IPSP and a long lasting hyperpolarization; these events are followed by a depolarizing rebound phase (Nuñez *et al.* 1993). The relative amplitude or even presence of the different components depends on the location and intensity of the stimulation. It was suggested that neocortical IPSPs *in vivo* are mainly due to an increased conductance to Cl^- ions activated by GABA released from interneurones (see Krnjevic, 1974). In order to compare spontaneous and evoked hyperpolarizations, we

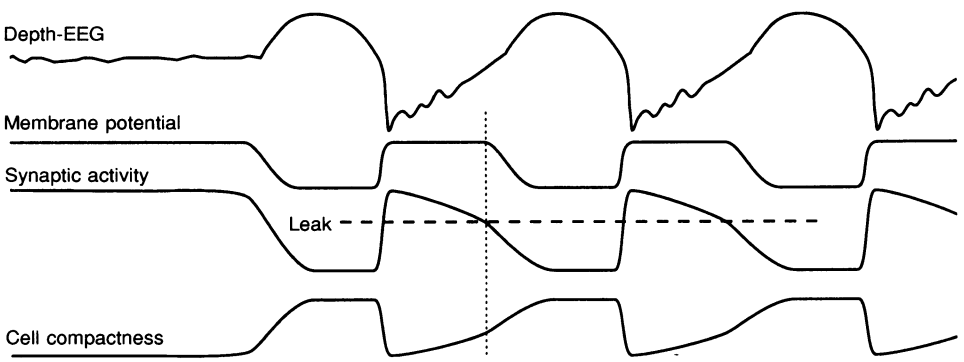

Figure 9. Scenario for the origin of slow sleep oscillations

Slow and synchronized oscillatory behaviour of cortical cells is reflected as stereotyped EEG components. The scheme is based on the balance of input synaptic currents of both excitatory and inhibitory nature (synaptic activity), leak currents (dotted line) that maintain the resting V_m, and the degree of compactness of the cell, here represented tentatively as the space constant of the cell. The threshold for the termination of each oscillatory cycle is determined by the crossing between I_{syn} and I_{leak} (dotted vertical line in the centre cycle).

constructed *V–I* curves for both. The spontaneous and the evoked long hyperpolarizations had curves with similar V_m range and slope (Fig. 3). This suggests that the underlying ionic mechanisms are similar and also suggests that $GABA_B$ IPSPs are not the dominant ionic mechanism underlying evoked long-lasting hyperpolarizations in Cx cells.

One may ask whether the fact that $GABA_B$ IPSPs are not apparent in our results is due to particular properties of GABA receptors in the motor cortex, compared with other brain regions. This does not seem to be the case as iontophoretic application of GABA gives remarkably similar responses in all neocortical regions in which it has been tested, including the motor cortex (Scharfman & Sarvey, 1987). Alternatively, the types and/or the distribution of interneurones in different neocortical regions might account for the difference. However, it is clear that this is not the case from *in vitro* studies done in the sensorimotor cortex which show clear $GABA_A$–$GABA_B$ responses to white matter stimulation (Connors *et al.* 1988).

One attractive explanation for the similarity between evoked and spontaneous hyperpolarizations is suggested by the convergence of different agonists upon the same K^+ channel. Adenosine, 5-HT and GABA have been shown to open the same pool of K^+ channels (Nicoll, Malenka & Kauer, 1990). It would then be possible to observe long-lasting hyperpolarizations that, although based on the same conductances, and therefore displaying similar *V–I* plots, would be triggered by different mechanisms during various physiological conditions. In this way, spontaneous hyperpolarizations could result from the action of adenosine (Haas & Greene, 1988) accumulated extracellularly during the depolarizing phase of the oscillation, while evoked hyperpolarizations could be triggered by $GABA_B$ receptors. However, we favour the explanation that the increase in conductance resulting from the activation of $GABA_B$ receptors is small compared with the considerable amount of excitatory synaptic inputs that are suddenly removed during the evoked hyperpolarizations. Therefore, although $GABA_B$ receptors are certainly involved in the generation of the evoked hyperpolarizations, their contribution is not the most important *in vivo*. Other examples of hyperpolarization due to disfacilitation have been described in spinal cord neurones (Llinás, 1964) and corticostriatal neurones (Cowan & Wilson, 1994).

It is important to mention that the stimulation used here represents a highly synchronized input to cortical and thalamic cells, and the elicited responses are only comparable with patterns observed during the states of slow-wave sleep, deep anaesthesia or epilepsy, bearing no relation to information processing during wakefulness.

RE cells

Evoked and spontaneous long-lasting hyperpolarizations in RE cells had similar *V–I* plots suggesting similar underlying mechanisms. There are no data available as to the ionic mechanisms underlying either one. Here too, withdrawal of synaptic inputs seems to be the mechanism dominating the membrane during both evoked and spontaneous hyperpolarizations. This hypothesis is supported by the lack of such long hyperpolarizations upon stimulation in ferret slices (Bal, von Krosigk & McCormick, 1995). In this respect RE cells resemble neostriatal neurones, in which cortically evoked long-lasting hyperpolarizations were shown to be due to disfacilitation (Wilson, Chang & Kitai, 1983).

TC cells

TC cells studied *in vitro* show a biphasic $GABA_A$–$GABA_B$ IPSP evoked by afferent stimulation (Crunelli *et al.* 1988). In the present study, as well as in previous *in vivo* studies (Paré, Curró Dossi & Steriade, 1991), these two types of GABA response were readily observed upon stimulation of cortical afferents or of the thalamus itself. TC cells also hyperpolarized spontaneously during the depth-positive phase of the oscillation. Importantly, however, in contrast to Cx and RE cells, an additional hyperpolarizing process, most probably a $GABA_B$ IPSP, was added onto the evoked hyperpolarization. This was clear from the *V–I* plots in which the V_m during the evoked hyperpolarization was obviously displaced towards more negative values. Thus, our data suggest that $GABA_B$ synaptic processes in TC cells are stronger than in the cortex. One possible explanation for this difference is the fact that RE cells mediate the generation of strong $GABA_B$ IPSPs since they display a particularly prolonged bursting behaviour (Domich *et al.* 1986; Steriade *et al.* 1986; Contreras *et al.* 1992; Huguenard & Prince, 1992; Destexhe & Sejnowski, 1996). Robust $GABA_B$ IPSPs are also apparent in thalamic nuclei devoid of RE inputs, such as the anterior nuclei (Paré *et al.* 1991). We favour the explanation that the difference between TC, RE and Cx is mostly due to the different distribution of the inhibitory inputs with respect to the somatic recording electrode. Thus, Cx and RE cells would have a more distributed $GABA_B$ inhibition on their extended dendritic arborizations, with smaller somatic current densities, compared with the more compact TC cells. Therefore, although $GABA_B$ responses are present in the three types of cells, they are not very evident in Cx and RE cells *in vivo*. We propose that this difference in the apparent strength of $GABA_B$ responses between TC and Cx cells increases the likelihood of rebound bursts in TC cells, thus favouring the thalamus as a site for pathological manifestations, such as some types of absence epilepsy.

Scenario for the generation of slow oscillations in large networks

During depth-negative phases of the slow oscillation, Cx and RE cells are depolarized, while TC cells display IPSPs generated by the spike bursts of RE cells. DC hyperpolarization in Cx and RE cells proved to be efficient in increasing the amplitude of the initial part of the depolarization, but also in reducing its final part, therefore reducing its duration. These data suggest that synaptic currents participating in building up the long depolarization

progressively run down, thus allowing the hyperpolarizing currents to take over. Supporting this hypothesis is the fact that the R_{in} increases progressively towards the following hyperpolarization.

In order to explain the initiation and termination of the hyperpolarizing phases that sculpture the slow oscillation, we propose the following scheme (Fig. 9).

Competition exists in every cell between synaptic currents (I_{syn}) and the passive leak currents (I_{leak}) for a stable resting V_m. I_{syn} is maintained at a high level by recurrent excitatory circuits, mostly corticocortical. Small decreases in I_{syn} will tend to allow I_{leak} to hyperpolarize the cell and decrease its firing probability. As more cells reduce their firing rates, I_{syn} would decrease concomitantly, creating a cascade reaction that leads to generalized neuronal silence. Thus, a critical number of cells must keep firing to sustain a large enough I_{syn}. During the long-lasting hyperpolarizations, as a consequence of the large decrease in I_{syn}, the space constant (λ) of the cell would increase, the cell becoming much more compact, being depolarized more easily and reaching firing threshold. Therefore, firing from any small group of cortical or thalamic cells would very rapidly bring the whole system back into the depolarizing state, which would explain the steeper uprising phase of the oscillatory cycles. Although no pacemaker cells seem to exist for the slow oscillation, both TC and Cx cells are capable of escaping from the long-lasting hyperpolarization and generating rebound excitation. In TC cells, the rebound bursts are more readily triggered at the end of the hyperpolarizations than in any other phase of the oscillation, thus contributing to the initiation of each oscillatory cycle. This suggestion is supported by the small overlap between steady-state activation and inactivation curves of the T current in TC cells (Coulter, Huguenard & Prince, 1989), indicating the existence of a tonically activated current in the range −60 to −70 mV that may bring the cell to the threshold of the LTS. The production of firing at the end of the hyperpolarizing phase is also due to the presence of the inward rectifier I_h (McCormick & Pape, 1990) that activates upon hyperpolarization and depolarizes the membrane. Cortical cells are certainly also capable of escaping from the hyperpolarization and trigger the oscillatory cycle, as demonstrated by the preservation of the slow oscillation after massive thalamic lesions (Steriade *et al.* 1993*c*).

One important theoretical consequence of the above scenario is that, besides the continuous synaptic bombardment from corticocortical and thalamocortical networks, a neuromodulator system is required to assure that small decreases in mean firing rate (as they indeed occur continuously) would not incidentally trigger a cascade of disfacilitation, rendering the system disconnected for a few hundreds of milliseconds. Indeed, activation of the mesopontine cholinergic system can selectively abolish the long-lasting hyperpolarizations of the slow oscillation (Steriade *et al.* 1993*a*). Moreover, transitions from brief episodes of EEG activation to an oscillatory state are always characterized by the initial appearance of synchronous, long-lasting hyperpolarizations in simultaneous intracellular recordings (Steriade *et al.* 1994*a*; Contreras & Steriade, 1995). Electrical stimulation would similarly generate a disfacilitation by synchronized activation of GABA IPSPs and hyperpolarizing currents such as $I_{K(Ca)}$, leading to an abrupt decrease in I_{syn}.

The exaggeration of this speculative picture by ketamine–xylazine anaesthesia, with high-amplitude positive and negative waves associated with hyper- and depolarizations in Cx and thalamic neurones, may be due to the combined effects of ketamine, which by blocking NMDA receptors (Anis, Berry, Burton & Lodge, 1983) increases the requirements of population firing rates to sustain an acceptable I_{syn}, and xylazine, which has hyperpolarizing actions itself, mediated by α_2-adrenoceptors (Nicoll *et al.* 1990). However, the present data are probably not only valid under the condition of ketamine–xylazine anaesthesia, as very similar EEG-cellular patterns of slow oscillation, with long-lasting and rhythmic (< 1 Hz) depth-EEG positive waves associated with silenced firing in Cx neurones, have recently been described during natural sleep in cats (Steriade *et al.* 1996).

Anis, N. A., Berry, S. C., Burton, N. R. & Lodge, D. (1983). The dissociative anaesthetics, ketamine and phencyclidine, selectively reduce excitation of central mammalian neurones by N-methyl-D-aspartate. *British Journal of Pharmacology* **79**, 565–575.

Avoli, M. (1986). Inhibitory potentials in neurons of the deep layers of the *in vitro* neocortical slice. *Brain Research* **370**, 165–170.

Bal, T., Von Krosigk, M. & McCormick, D. A. (1995). Role of the ferret perigeniculate nucleus in the generation of synchronized oscillations *in vitro*. *Journal of Physiology* **483**, 665–685.

Connors, B. W., Malenka, R. C. & Silva, L. R. (1988). Two inhibitory postsynaptic potentials, and $GABA_A$ and $GABA_B$ receptor-meditated responses in neocortex of rat and cat. *Journal of Physiology* **406**, 443–468.

Contreras, D., Curró Dossi, R. & Steriade, M. (1993). Electrophysiological properties of cat reticular thalamic neurones *in vivo*. *Journal of Physiology* **470**, 273–294

Contreras, D. & Steriade, M. (1995). Cellular bases of the EEG slow rhythms: a study of dynamic corticothalamic relationships. *Journal of Neuroscience* **15**, 604–622.

Coulter, D. A., Huguenard, J. R. & Prince, D. A. (1989). Calcium currents in rat thalamocortical relay neurones: kinetic properties of the transient, low-threshold current. *Journal of Physiology* **414**, 587–604.

Cowan, R. L. & Wilson, C. J. (1994). Spontaneous firing patterns and axonal projections of single corticostriatal neurons in the rat medial agranular cortex. *Journal of Neurophysiology* **71**, 17–32.

Crunelli, V. N., Haby, M., Jassik-Gerschenfeld, D., Leresche, N. & Pirchio, M. (1988). Cl^-- and K^+-dependent inhibitory postsynaptic potentials evoked by interneurones of the rat lateral geniculate nucleus. *Journal of Physiology* **399**, 153–176.

DESTEXHE, A. & SEJNOWSKI, T. J. (1996). G protein activation kinetics and spillover of gamma-aminobutyric acid may account for differences between inhibitory responses in the hippocampus and thalamus. *Proceedings of the National Academy of Sciences of the USA* **92**, 9515–9519.

DOMICH, L., OAKSON, G. & STERIADE, M. (1986). Thalamic burst patterns in the naturally sleeping cat: a comparison between cortically projecting and reticularis neurones. *Journal of Physiology* **379**, 429–450.

EVARTS, E. V. (1964). Temporal patterns of discharge of pyramidal tract neurons during sleep and waking in the monkey. *Journal of Neurophysiology* **27**, 152–171.

HAAS, H. L. & GREENE, R. W. (1988). Endogenous adenosine inhibits hippocampal CA1 neurones: further evidence from extra- and intracellular recording. *Archives of Pharmacology* **337**, 561–565.

HALLIWELL, J. V. (1986). M-current in human neocortical neurons. *Neuroscience Letters* **67**, 1–6.

HUGUENARD, J. R. & PRINCE, D. A. (1992). A novel T-type current underlies prolonged Ca^{2+}-dependent burst firing in GABAergic neurons of the rat thalamic reticular nucleus. *Journal of Neuroscience* **12**, 3804–3817.

KELLY, J. S., KRNJEVIC, K., MORRIS, M. E. & YIM, G. K. W. (1969). Anionic permeability of cortical neurones. *Experimental Brain Research* **7**, 11–31.

KRNJEVIC, K. (1974). Chemical nature of synaptic transmission in vertebrates. *Physiological Reviews* **54**, 418–450.

LLINÁS, R. (1964). Mechanisms of supraspinal action upon spinal cord activities. Differences between reticular and cerebellar inhibitory action upon alpha extensor motorneurons. *Journal of Neurophysiology* **27**, 1117–1126.

MCCARLEY, R. W., BENOIT, O. & BARRIONUEVO, G. (1983). Lateral geniculate nucleus unitary discharge in sleep and waking: state- and rate-specific aspects. *Journal of Neurophysiology* **50**, 798–818.

MCCORMICK, D. A. (1989). GABA as an inhibitory neurotransmitter in human cerebral cortex. *Journal of Neurophysiology* **62**, 1018–1027.

MCCORMICK, D. A., CONNORS, B. W., LIGHTHALL, J. W. & PRINCE, D. A. (1985). Comparative electrophysiology of pyramidal and sparsely spiny stellate neurons of the neocortex. *Journal of Neurophysiology* **54**, 782–806.

MCCORMICK, D. A. & PAPE, H. C. (1990). Properties of a hyperpolarization-activated cation current and its role in rhythmic oscillations in thalamic relay neurones. *Journal of Physiology* **431**, 291–318.

NICOLL, R. A., MALENKA, R. C. & KAUER, J. (1990). Functional comparison of neurotransmitter receptor subtypes in mammalian central nervous system. *Physiological Reviews* **70**, 513–565.

NUÑEZ, A., AMZICA, F. & STERIADE, M. (1993). Electrophysiology of cat association cortical cells *in vivo*: intrinsic properties and synaptic responses. *Journal of Neurophysiology* **70**, 418–429.

PARÉ, D., CURRÓ DOSSI, R. & STERIADE, M. (1991). Three types of inhibitory postsynaptic potentials generated by interneurons in the anterior thalamic complex of cat. *Journal of Neurophysiology* **66**, 1190–1204.

POLLEN, D. A. & LUX, H. D. (1965). Conductance changes during inhibitory postsynaptic potentials in normal and strychninized cortical neurones. *Journal of Neurophysiology* **29**, 369–381.

RENAUD, L. P., KELLY, J. S. & PROVINI, L. (1974). Synaptic inhibition in pyramidal tract neurons: membrane potential and conductance changes evoked by pyramidal tract and cortical surface stimulation. *Journal of Neurophysiology* **37**, 1144–1155.

SCHARFMAN, H. E. & SARVEY, J. M. (1987). Responses to GABA recorded from identified rat visual cortical neurons. *Neuroscience* **23**, 407–422.

SCHWINDT, P. C., SPAIN, J. W. & CRILL, W. E. (1989). Long-lasting reduction of excitability by a sodium-dependent potassium current in cat neocortical neurons. *Journal of Neurophysiology* **61**, 233–244.

SCHWINDT, P. C., SPAIN, J. W., FOEHRING, R. C., STAFSTROM, C. E., CHUBB, M. C. & CRILL, W. E. (1988). Multiple potassium conductances and their functions in neurons from cat sensorimotor cortex. *Journal of Neurophysiology* **59**, 424–449.

STEFANIS, C. & JASPER, H. (1964). Intracellular microelectrode studies of antidromic response in cortical pyramidal tract neurons. *Journal of Neurophysiology* **27**, 828–854.

STERIADE, M., AMZICA, F. & CONTRERAS, D. (1996). Synchronization of fast (30–40 Hz) spontaneous cortical rhythms during brain activation. *Journal of Neuroscience* **16**, 392–417.

STERIADE, M., AMZICA, F. & NUÑEZ, A. (1993*a*). Cholinergic and noradrenergic modulation of the slow (≈ 0·3 Hz) oscillation in neocortical cells. *Journal of Neurophysiology* **70**, 1385–1400.

STERIADE, M., CONTRERAS, D. & AMZICA, F. (1994). Synchronized sleep oscillations and their paroxysmal developments. *Trends in Neurosciences* **17**, 199–208.

STERIADE, M., CONTRERAS, D., CURRÓ DOSSI, R. & NUÑEZ, A. (1993*b*). The slow (< 1 Hz) oscillation in reticular thalamic and thalamocortical neurons: scenario of sleep rhythm generation in interacting thalamic and neocortical networks. *Journal of Neuroscience* **13**, 3284–3299.

STERIADE, M., DESCHENES, M. & OAKSON, G. (1974). Inhibitory processes and interneuronal apparatus in motor cortex during sleep and waking. I. Background firing and responsiveness of pyramidal tract neurons and interneurons. *Journal of Neurophysiology* **37**, 1065–1092.

STERIADE, M., DOMICH, L. & OAKSON, G. (1986). Reticularis thalamic neurons revisited: activity changes during shifts in states of vigilance. *Journal of Neuroscience* **6**, 68–81.

STERIADE, M., NUÑEZ, A. & AMZICA, F. (1993*c*). A novel slow (< 1 Hz) oscillation of neocortical neurons *in vivo*: depolarizing and hyperpolarizing components. *Journal of Neuroscience* **13**, 3252–3265.

STERIADE, M., NUÑEZ, A. & AMZICA, F. (1993*d*). Intracellular analysis of relations between the slow (< 1 Hz) neocortical oscillation and other sleep rhythms of the electroencephalogram. *Journal of Neuroscience* **13**, 3266–3283.

WILSON, C. J., CHANG, H. T. & KITAI, S. T. (1983). Disfacilitation and long lasting inhibition of neostriatal neurons in the rat. *Experimental Brain Research* **51**, 227–235.

Acknowledgements

This work was supported by grant MT-3689 from the Medical Research Council of Canada. D.C. is a PhD student and I.T. a postdoctoral fellow. We thank A. Destexhe for helpful discussions and P. Giguère and D. Drolet for technical assistance.

Author's email address

M. Steriade: mircea.steriade@phs.ulaval.ca

Received 9 October 1995; 19 February 1996.